2005

Importance of Cations in the Properties of Zintl Phases: The Electronic Structure of and Bonding in Metallic Na6TlSb41

Anja V. Mudring
Universität zu Köln, mudring@iastate.edu

John D. Corbett
Iowa State University

Importance of Cations in the Properties of Zintl Phases: The Electronic Structure of and Bonding in Metallic Na6TlSb41

Abstract

The novel metallic compound Na_6TlSb_4 consists of four-membered $TlSb_3$ rings joined by pairs of Sb atoms into Tl_2Sb_8 units, the last of which is further interconnected into 1D anionic chains via Tl–Tl bonds. The contrast of its metallic conductivity with that of the $2 - e^-$ poorer, electron precise, and semiconducting Zintl phase $K_6Tl_2Sb_3$, which has virtually the same anionic network, has been investigated by ab initio LMTO-DFT methods. Sodium ion participation is found to be appreciable in the (largely) Sb *p* valence band and especially significant in an additional low-lying conduction band generated by antimony pπ and sodium orbitals. The one pyramidal 3-bonded Sb atom appears to be largely responsible for the interchain conduction process. The substitution of one Tl by Sb, which occurs when the countercation is changed from potassium in $K_6Tl_2Sb_3$ to sodium, yielding only Na_6TlSb_4, is driven by a distinctly tighter packing, a corresponding increase in the Madelung energy, and binding of the excess pair of electrons in the new conduction band.

Disciplines

Electromagnetics and Photonics | Metallurgy | Other Electrical and Computer Engineering | Other Materials Science and Engineering

Comments

Reprinted with permission from Inorg. Chem., 2005, 44 (16), pp 5636–5640.

Inorg. Chem. **2005**, *44*, 5636–5640

Importance of Cations in the Properties of Zintl Phases: The Electronic Structure of and Bonding in Metallic Na_6TlSb_4[1]

Anja-V. Mudring[†,‡] **and John D. Corbett***[,‡]

Institut für Anorganische Chemie der Universität zu Köln, Greinstr. 6, D-50939 Köln, Germany, and Ames Laboratory—U.S. Department of Energy, and Department of Chemistry, Iowa State University, Ames, Iowa 50011

Received January 26, 2005

The novel metallic compound Na_6TlSb_4 consists of four-membered $TlSb_3$ rings joined by pairs of Sb atoms into Tl_2Sb_8 units, the last of which is further interconnected into 1D anionic chains via Tl–Tl bonds. The contrast of its metallic conductivity with that of the $2 - e^-$ poorer, electron precise, and semiconducting Zintl phase $K_6Tl_2Sb_3$, which has virtually the same anionic network, has been investigated by ab initio LMTO-DFT methods. Sodium ion participation is found to be appreciable in the (largely) Sb *p* valence band and especially significant in an additional low-lying conduction band generated by antimony pπ and sodium orbitals. The one pyramidal 3-bonded Sb atom appears to be largely responsible for the interchain conduction process. The substitution of one Tl by Sb, which occurs when the countercation is changed from potassium in $K_6Tl_2Sb_3$ to sodium, yielding only Na_6TlSb_4, is driven by a distinctly tighter packing, a corresponding increase in the Madelung energy, and binding of the excess pair of electrons in the new conduction band.

1. Introduction

Historically, studies of Zintl phases have mainly focused on the anionic substructures. This originated from the simple view that cations in Zintl phases transfer their electrons onto the anions which in turn form ideal substructures that can be well explained by simple guidelines for stable electron counts, such as Zintl–Klemm, octet, or Wade's rules.[2] Accordingly, it would be expected that filled anion-centered orbitals will lie well separated from the empty cation-based energy levels at higher energies and that the materials in consequence would be insulators or at least semiconductors. This should be especially true for the commonly involved alkali metals Na–Cs. Thus, the examination of the physical properties of supposed Zintl phases in the past has been neglected to a great extent, but recently, more and more examples of supposed Zintl phases have been identified that violate such simple views of bonding.[3,4] We have recently given theoretical attention to some of these problems at the ab initio level.[5–7]

The present article concerns another problem, but one of a different character, Na_6TlSb_4, for which the structure and properties have been recently reported.[8] Na_6TlSb_4 belongs to a growing class of ternary main-group pnictide salts that often exhibit characteristic low-dimensional anionic frameworks. Assuming localized $2c-2e$ bonds within the anionic network, this compound has two electrons (and two cations) more than the number required for its connectivity, in perfect agreement with the metallic conductivity found. The valence composition Na_4TlSb_4 cannot be obtained in any structure. This result is in notable contrast to the more conventional Zintl phase $K_6Tl_2Sb_3$, which has virtually the same anionic framework[9] but with one more Tl and one fewer Sb atom per anion chain unit is electron precise. Accordingly, $K_6Tl_2Sb_3$ behaves as a semiconductor with $\rho_{298} = \sim 0.77$ mΩ

* To whom correspondence should be addressed. Email: jcorbett@iastate.edu.
† University of Cologne.
‡ Iowa State University.

(1) This research was supported in part by the Office of the Basic Energy Sciences, Materials Science Division, U.S. Department of Energy (DOE). The Ames Laboratory is operated by the Iowa State University under Contract No. W-7405-Eng-82.

(2) *Chemistry, Structure and Bonding of Zintl Phase and Ions*; Kauzlarich, S. M., Ed.; VCH: New York, 1996.
(3) Corbett, J. D. In *Chemistry, Structure and Bonding of Zintl Phase and Ions*; Kauzlarich, S. M. Ed.; VCH: New York, 1996; Chapter 3.
(4) Corbett, J. D. *Angew. Chem., Int. Ed.* **2000**, *39*, 670.
(5) Mudring, A.-V.; Corbett, J. D. *Z. Anorg. Allg. Chem.* **2002**, *628*, 2226.
(6) Mudring, A.-V.; Corbett, J. D. *J. Am. Chem. Soc.* **2004**, *126*, 5277.
(7) Guloy, A. M.; Mudring, A.-V.; Corbett, J. D. *Inorg. Chem.* **2003**, *42*, 6673.
(8) Li, B.; Chi, L.; Corbett, J. D. *Inorg. Chem.* **2003**, *42*, 3036.
(9) Chi, L.; Corbett, J. D. *Inorg. Chem.* **2001**, *40*, 2705.

10.1021/ic050128n CCC: $30.25
Published on Web 07/12/2005

cm. The contrast is now more evident: in the presence of the smaller more tightly bound sodium cations it becomes energetically favorable to add and delocalize two additional electrons via a parallel Tl ⟹ Sb substitution. The nature of the resulting conduction state remains an unanswered question. A growing number of what might be called "metallic Zintl phases" or, alternatively, phases that bind extra cations and electrons are known.[3,4]

Extended Hückel calculations are commonly carried out to explain the electronic behavior of compounds composed of alkali metal cations and clusters and networks of main group elements around and beyond the Zintl border. Because of the lack of good orbital parameters for alkali metals in Hückel calculations, these generally get neglected; although, by chemical intuition, they are usually considered to be of no importance anyway because the anionic substructures seem to govern the covalently bonded structure and the properties of these materials. However, recent studies have shown how important it is to take the higher-charged alkaline earth metal cations into account for situations in which the electronic structure of supposed Zintl phases is being studied.[5,7] Na_6TlSb_4 is another example for which simple Hückel theory fails to properly describe the bonding situation, presumably because of the neglect of cation roles. Therefore, a more thorough theoretical exploration of the electronic structure of this compound is of eminent interest. An abstract of the results has appeared.[10]

2. Experimental Section

Computational Details. Semiempirical extended Hückel calculations (EH) for the whole $(TlSb_4)_n$ network were performed using the CAESAR[11] program package with the following parameters: H_{ij} (eV) (ζ_1) Tl 6*s* −18.0 (2.679), 6*p* −12.7 (2.322); Sb 5*s* −4.34 (0.874), 5*p* −2.73 (0.874).[11] 1D Tl−Sb chains automatically result without Na atom participation in the bonding.

A thorough investigation of the electronic structure of Na_6TlSb_4 was also carried out by the tight-binding linear-muffin-tin-orbital (LMTO) method[12] in the local density (LDA, Barth−Hedin functional) and atomic sphere (ASA) approximations, within the framework of the DFT method.[13] Four interstitial spheres are introduced in the last step to achieve space filling (muffin-tin radii r = 3.90, 1.6 (×3) Å; only 1s-like wave functions are taken into account during calculations, 2s is treated by downfolding techniques, and higher functions are omitted). The ASA radii, as well as the positions and radii of additional empty spheres, are calculated automatically. Reciprocal space integrations are carried out using the tetrahedron method.[14] Twelve irreducible k points were used in the 3D calculations. The basis set of short-ranged atom-centered TB-LMTOs contain *n*s, *n*p, *n*d, and (n − 1)f wave functions for Sb (n = 5) and Tl (n = 6). The d and f orbitals are treated with the downfolding technique[15] (muffin-tin radius for Tl is 3.22 Å; for Sb the values range from 3.33 to 3.66 Å). For sodium, 3s, 3p, and 3d are taken into account as valence orbitals, the latter two again being treated by the downfolding technique; their muffin-tin radii range from 3.52 to 3.73 Å. For bond analysis, the crystal orbital Hamiltonian population (COHP) method is used.[16] COHP gives the energy contributions for all electronic states of selected bonds by partitioning the band structure energy in terms of the respective orbital pair contributions. The structural data employed are as reported.[8]

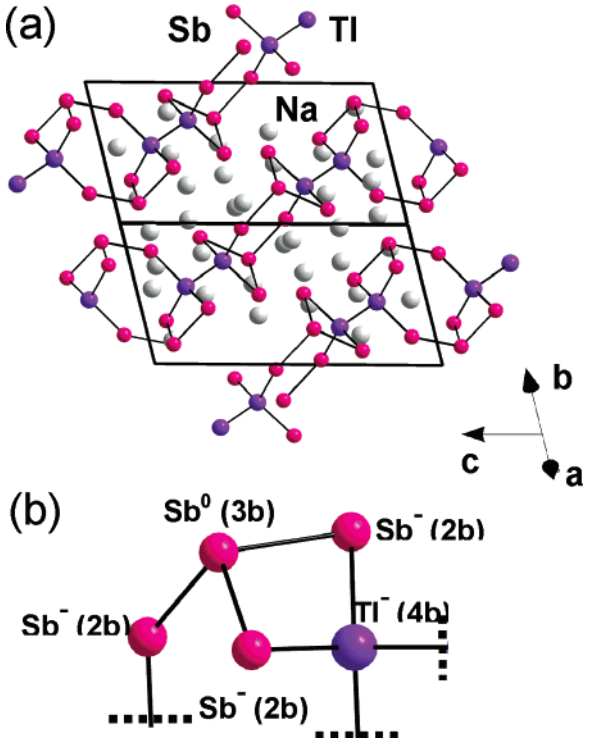

Figure 1. (a) Representation of the crystal structure of Na_6TlSb_6 (Na, light gray; Sb, magenta; Tl, purple). (b) Representation of the smallest repeat unit in the anionic $[^1_\infty Sb_4Tl]$ strands with the formal oxidation state marked for each atom according to an octet treatment.

3. Results and Discussion

The structure of Na_6TlSb_4 is characterized by four-membered $TlSb_3$ rings that are interlinked by pairs of Sb bridges to generate swinglike repeating units of $[Tl_2Sb_8]$, and these are further interconnected by external Tl−Tl bonds into infinite one-dimensional chains, Figure 1a. One set of the independent atom types is labeled (Sb, red; Tl, purple; Na, light gray). Figure 1b shows the smallest repeat unit in which the atoms are now distinguished by function, namely as one three-bonded antimony (3b-Sb^0, Sb4), three two-bonded antimony (2b-Sb^-), and one four-bonded thallium atom (Tl^-). The assigned oxidation states reflect the requirements of the octet rule and 2c−2e bonding and show that the repeat unit in Na_6TlSb_4 contains two excess electrons per formula unit (6 − 0 − 3(1) − 1, respectively). This is in perfect agreement

(10) Mudring, A.-V.; Corbett, J. D. *Z. Anorg. Allg. Chem.* **2004**, *630*, 1746.
(11) Ren, J.; Liang, W.; Whangbo, M.-H. *CAESAR*; PrimeColor Software Inc.: Raleigh, NC, 1998.
(12) (a) Shriver, H. L. *The LMTO Method*; Springer-Verlag: Berlin, Germany, 1984. (b) Jepsen, O.; Snob, M.; Andersen, O. K. *Linearized Band-Structure Methods in Electronic Band-Structure and its Applications*; Springer Lecture Note; Springer-Verlag: Berlin, Germany, 1987. (c) Anderson. O, K.; Jepsen, O. *Phys. Rev. Lett.* **1984**, *53*, 2571.
(13) Tank, R. W.; Jepsen, O.; Burckhardt. A.; Andersen, O. K. *TB-LMTO-ASA Program*, version 4.7; Max-Planck-Institut für Festkörperforschung: Stuttgart, Germany, 1998.
(14) Andersen, O. K.; Jepsen, O. *Solid State Commun.* **1971**, *9*, 1763. (b) Blöchl, P.; Jepsen, O.; Andersen, O. K. *Phys. Rev. B.* **1994**, *34*, 16223.
(15) Lambrecht, W. R. L.; Andersen, O. K. *Phys. Rev. B* **1986**, *B34*, 2439. (b) Jepsen, O.; Andersen, O. K. *Z. Phys.* **1995**, *B97*, 35. (c) Krier, G.; Jepsen, O.; Andersen, O, K. Max-Planck-Institute fur Festkörperforschung, Stuttgart, Germany, Unpublished.
(16) Dronskowski, R.; Blöch, P. *J. Phys. Chem.* **1993**, *97*, 8617.

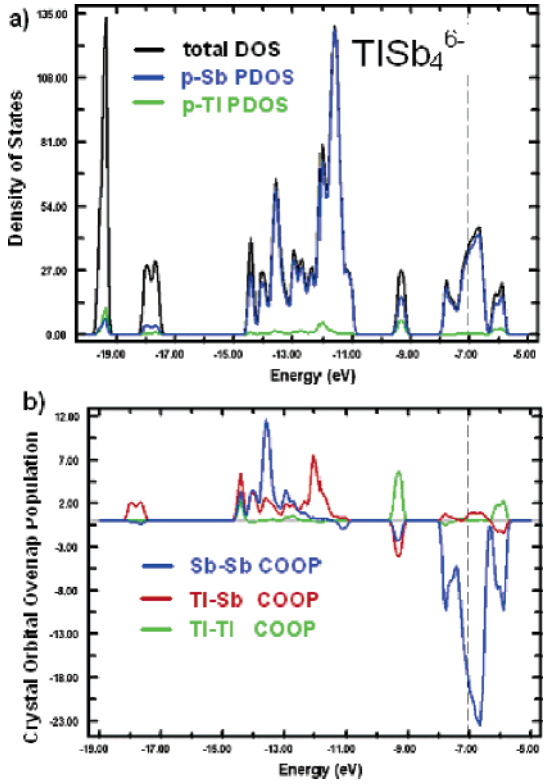

Figure 2. Graphical representation of the results of an extended Hückel calculation for $[^1_\infty Sb_4Tl]^{6-}$. (a) Total densities of states (DOS) in black with projected densities of states (PDOS) for Sb p (blue) and Tl p (green). (b) Crystal orbital overlap population (COOP) plots for selected interactions: Sb−Sb (blue), Tl−Sb (red), and Tl−Tl (green).

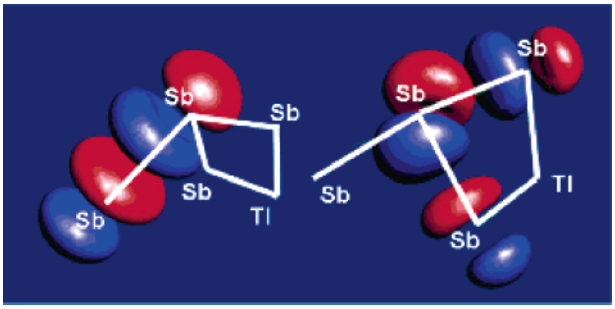

Figure 3. Localized molecular orbital HOMO (highest-occupied molecular orbital) and HOMO-1 depicting the antibonding F situation just below the Fermi level in Na_6TlSb_4 according to EHMO treatment (Figure 2).

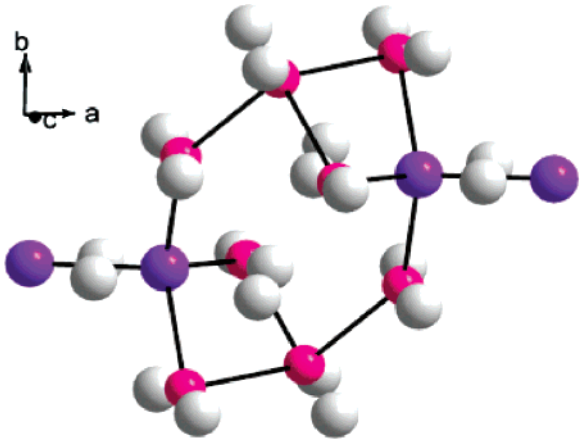

Figure 4. Projection of the Na_6TlSb_4 structure roughly normal to the central ring in the chain. Note the location of the sodium atoms (light gray) with respect to the Sb and Tl atoms.

with the measured (isotropic) metallic conductivity, $\rho_{295} = 0.054$ mΩ cm with $d\rho/dT = 0.72\%$ K^{-1}.[8]

The problem was first examined by a simple extended Hückel calculation on the $[^1_\infty TlSb_4^{6-}]$ chain which omits any role for the sodium cations. The densities of states (Figure 2a) are made up of, from low to high energies, Tl s states, Sb s states, and a large band of largely Sb p states. The Tl p contributions are spread out over the range with a distinct peak at ∼−9 eV that has Sb p as well as Tl p contributions. More antimony p levels are again found around the Fermi level, but no significant densities of states (DOS) were found for thallium. Interpretation of the chemical bonding within the anion using Crystal Orbital Overlap Population (COOP) analysis (Figure 2b) shows strong Sb−Sb as well as Sb−Tl bonds in the region of −11 to −15 eV, followed by a narrow Tl−Tl bonding band near −9.5 eV that is also Sb−Sb as well as Sb−Tl antibonding. Around the Fermi level a large number of nominally σ antibonding Sb−Sb interactions are formed by Sb p state interactions. Figure 3 shows the shapes of the two localized antibonding F interactions just below E_F to emphasize the improbable nature of this bonding picture.

The question of how the conduction electrons travel in this material must be answered. Note that electronic conductivity along the $[^1_\infty Sb_4Tl]$ chain through the Tl−Tl or Tl−Sb bonds is impossible as thallium does not contribute to the DOS around the Fermi level, and there are no short Sb−Sb distances around that bond. The need for interchain communication and an additional low-lying open band for the extra electrons composed mainly of bonding states is manifest. There are clearly open but antibonding Sb−Sb states near Fermi in the anion alone (Figure 2), and so sodium participation seems to be a necessity. A provocative structural hint concerning the solution comes from an alternate view of a portion of the structure roughly normal to the independent ring shown in Figure 4 in which the sodium atoms are seen to be situated more-or-less above and below all of the antimony atoms near what would be imagined to be their π states. This does not apply to 4-bonded Tl in the dimers, instead sodium is centered alongside the presumed Tl−Tl σ bond in this case. Significant electrostatic Na−Tl interactions and fewer cation−cation repulsions were earlier postulated to account for the 0.26 Å shorter Tl−Tl bond in this salt than in $K_6Tl_2Sb_3$.[8] We have accordingly undertaken a more thorough theoretical treatment of Na_6TlSb_4 via 3D ab initio DFT-LMTO-ASA calculations including the sodium cations.

The DOS values obtained from these studies are shown in Figure 5 with projected DOS contributions by (a) Sb (red), (b) Tl (green), and (c) Na (blue). These reflect the basic features found according to semiempirical Hückel calculations (Figure 2) but with some notable differences: stronger splitting of the Tl−Tl bonding/antibonding states and, most importantly, substantial contributions from sodium states. The sodium contributions are notable in both the mostly Sb valence band around ∼−1.2 to −4 eV and a separate conduction band from about −1.0 eV to above E_F. The

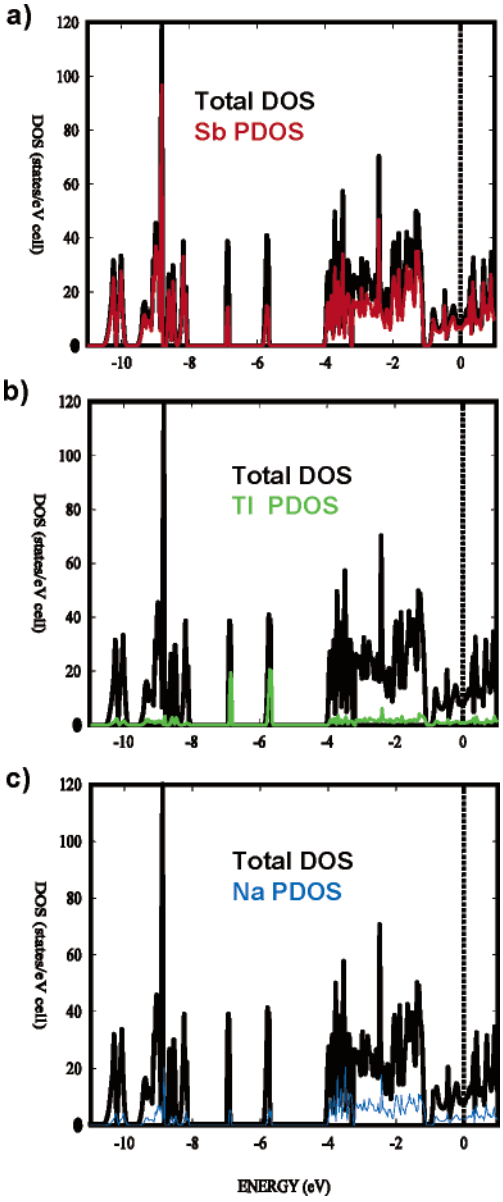

Figure 5. Graphical representation of the results of ab initio DFT-LMTO-ASA studies of Na_6TlSb_4 with the total densities of states (DOS) in black plus projected densities of states (PDOS) for (a) Sb (red), (b) Tl (green), and (c) Na (blue).

Table 1. Integrated (−COHP) Values, by Atom (eV/cell)

to all Na		to all Sb	
Sb1	2.83	Na1	1.53
Sb2	3.00	Na2	1.70
Sb3	2.98	Na3	1.77
Sb4	1.03	Na4	1.76
Tl	0.64	Na5	1.68
		Na6	1.65

specific contributions were sorted out with the aid of COHP calculations for each of the four antimony atoms with all sodium atoms, for Tl with sodium, and for each of the six sodium atoms with all antimony atoms. Plots of all of these data are contained in the Supporting Information. The integrated COHP energy totals, up to E_F, are also given in Table 1. The one unique Sb(x)−Na COHP behavior is shown in Figure 6 for the distinctive 3-bonded Sb4 (Sb^0), which exhibits significant antibonding effects in the upper valence

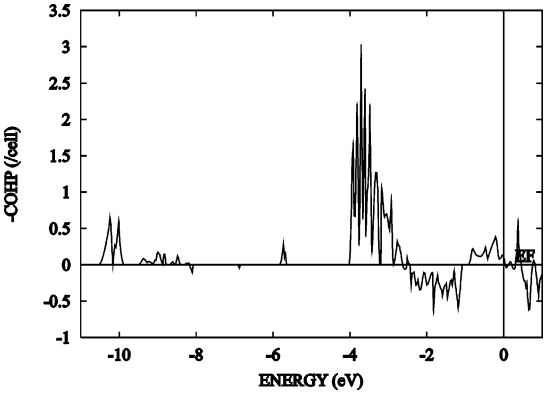

Figure 6. Crystal orbital Hamiltonian population (COHP) plot for the 3-bonded Sb4 interactions with Na (Sb^0−Na, Figure 1b).

band (and a smaller −COHP value) as well as the most prominent Sb−Na bonding at relatively low energies in the new conduction band. These effects appear to be associated with the unique character and environment of the bonding about the pyramidal Sb4 atom, which will be considered shortly. Corresponding COHP plots for each of the other 2-bonded Sb1, Sb2, and Sb3 atoms with all of the Na atoms demonstrate (a) somewhat larger Sb(x)−Na bonding in the upper half of the valence band and (b) smaller but still principally bonding effects in the conduction band below E_F. The last differences are presumably the result of these more negative (formally Sb^{1-}) atoms exhibiting less covalent bonding. Fat band representations for sodium contributions to the bands (Supporting Information) illustrate the general and significant involvement of sodium in most of the valence (Sb p) band and above without providing much more useful information for the present analysis except to call attention to the fact that Fermi energy crossings occur in nine regions of k space, making it clear that we are dealing with 3D conduction.

The integrated −I(COHP) data for the Sb_x−Na and Na_x−Sb combinations listed in Table 1 show that all are rather uniformly strong except as already noted. Despite the rather complex structure, some additional conclusions can be drawn regarding the interchain interactions, the distinctive overall bonding of 3-bonded Sb4, and the somewhat lower −I(COHP) result for Na1. The shortest interchain Sb−Sb distances along with very clear Na interbridging are found for Sb4, perhaps not surprising considering the distinctive pyramidal bonding of this atom in the ring (internal angles of ∼102°). Its nonbonded nearest neighbors in adjoining chains are Sb1, Sb2, and Sb3 at 4.40, 4.29, and 4.28 Å, respectively, in contrast with both the next nearest intra- and interchain Sb−Sb distances (d(Sb−Sb)) of 4.97 Å for Sb1−Sb3 in the four-membered rings and 4.97 Å and up (Sb2−Sb4, Sb1−Sb3) and 2.99−3.25 Å in the rings.

The earlier discussion of the structure[8] noted that the cation placements are very good evidence for an outward directed lone pair on Sb4, namely, a substantial open volume defined by the three nearest-neighboring cations in an outward direction, Na2, Na3, and Na5, which are separated from each other by 5.15 Å and up. (The shorter Na−Na bond distances elsewhere in the structure fall in the range of 3.45−3.75 Å.)

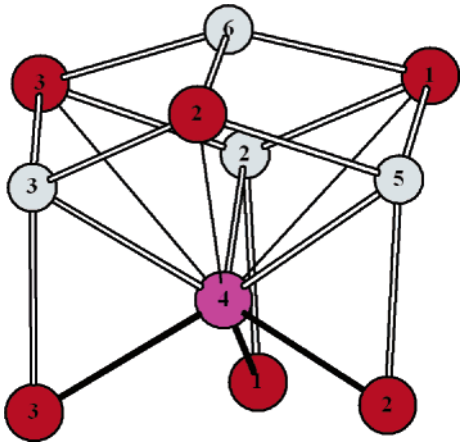

Figure 7. Geometric environment of the unique Sb4 (lavender), which is bonded within the ring to the lower Sb1, Sb2, and Sb3 atoms (3.22−3.25 Å) and distantly to the Sb1, Sb2, and Sb3 atoms in two other chains above (light lines) (at 4.20−4.28 Å) via intervening Na2, Na3, and Na5 atoms (d(Sb−Na) = 3.20−3.25 Å). The Na6 cap is 3.83 Å from Sb4. The upper Na and Sb atoms appear to give good definition of a cavity presumably occupied by a lone pair of electrons on Sb4.

These three Na cations are also intimately associated with the short linkage of Sb4 to Sb1, Sb2, and Sb3 in other chains noted above, as illustrated in Figure 7 (three more close Na atoms about Sb4 lie at quite low angles). The Sb4 (lavender) is bonded to the lower ring atoms, Sb1, Sb2, and Sb3 (red), at typical 3.22−3.25 Å distances, whereas the neighboring Sb1, Sb2, and Sb3 (red) atoms in other chains noted above occur at longer distances, 4.40−4.28 Å (thin lines). The intervening Na2, Na3, and Na5 (light gray) atoms are specially oriented to eclipse the bottom Sb1, Sb2, and Sb3 atoms, respectively, with short 3.25−3.20 Å separations, among the shorter d(Sb−Na) in the structure (a distance matrix is in Supporting Information). The upper triangle of well-separated Sb1, Sb2, and Sb3 atoms are likewise close to the same three intervening Na cations at 3.20−3.35 Å, and the array is precisely capped by an axial Na6 atom that is 3.83 Å from Sb4. These last three Sb atoms occur in two different chains: the Sb2−Sb3 pair falls across a Tl−Tl bond in one. It is probable that the highly directional lone pair evident on Sb4 and the greater Sb−Na covalencies with this less reduced Sb are responsible for some antibonding effects with Na (Figure 6). In contrast, the sodium distributions about the other three Sb atoms in the rings show no spatial evidence for any highly directional lone pairs of elections.

To the extent that we can infer bond strengths from distances, the lower −I(COHP) value for Na1 (Table 1) is also consistent with its location, as it appears to be the least well bonded. The Tl_2Sb_8 rings within the chains are all centric, and Na1 lies directly above and below each ring, tightly bound (at ∼3.22 Å) to a pair of trans Sb2 atoms but more weakly bound to the points of the four-membered rings at either end, Sb1 and Sb3 (3.49, 3.50 Å), with no other Sb neighbors at <4.10 Å. The Sb2 neighbors are strongly bound into the Na network (Table 1).

This theoretical study also allows us some more insights and understanding of the differences between the structure discussed above and the structure of $K_6Tl_2Sb_3$. These analogous chains have somewhat different conformations as they run in a different direction normal to $\vec{b}$ in the same $C2/c$ space group, which places 2-fold axes instead of inversion points in the centers of the rings. The most striking feature of the conversion of this to Na_6TlSb_4 is the substantial volume contraction on its formation, 730 Å^3 per formula unit, which is 57% greater than the value estimated on the basis of standard volume differences between K and Na (together with much smaller terms for Tl vs Sb volumes in other intermetallics). Some of this follows from the 0.26 Å contraction in the Tl−Tl bond length which appears to result largely from the reduction in the van der Waals volumes of six K atoms vs six Na atoms that lie around the Tl−Tl bonds.[8] The cation−Sb distances elsewhere in the structures range around 3.80 (K) vs 3.45 Å (Na). Some more of the spontaneity must be associated with the tighter packing, the corresponding gain in Madelung energies, and the enhanced Na−Sb bonding that is generated in the alternate packing and delocalization in a rather tightly packed though complex structure.

This novel phase Na_6TlSb_4 is thus another example of a Zintl phase in which it is essential to take the cations into account when considering the compound's properties even when these are as "inert" as sodium might be presumed to be. The inclusion of extra bound electrons and cations in stable products has been encountered with increasing frequency in recent years,[3,4] for example in what may be written as $K_8In_{11}e^-$,[17−19] $K_8Tl_{11}e^-$,[20] $K_3Bi_2e^-$,[21] and $Sr_3Sn_5(e^-)_2$.[22] A general increase in Madelung energy contributions accompany binding of these extra cations, and although the consequent metallic characteristics have been frequently acknowledged, more specific details about the status of the extra electrons have generally been lacking. A related but somewhat different situation for K_5Bi_4 has been well considered recently.[23]

Acknowledgment. A.-V.M. would like to acknowledge the Alexander von Humboldt Foundation for a Lynen fellowship that helped support a research stay at the Ames Laboratory and the Fonds der Chemischen Industrie for a Liebig fellowship. Enric Canadell has provided helpful discussions and insights regarding the problem considered here.

Supporting Information Available: A distance matrix for Sb−Na and nonbonding Sb−Sb interactions, COHP plots for the interaction of each Sb, Tl, and Na with all of the other kind of atom in Na_6TlSb_4, a fat-band representation of Na contributions to the band structure, and a more detailed drawing of the environment around Sb4. This material is available free of charge via the Internet at http://pubs.acs.org.

IC050128N

(17) Sevov, S. C.; Corbett, J. D. *Inorg. Chem.* **1991**, *30*, 4875.
(18) Blase, W.; Cordier, G.; Müller, V.; Häussermann, U.; Nesper, R. *Z. Naturforsch.* **1993**, *48b*, 754.
(19) Llusar, R.; Beltrán, A.; Andres, J.; Silvi, B.; Sevin, A. *J. Phys. Chem.* **1995**, *99*, 521.
(20) Dong, Z.-C.; Corbett, J. D. *J. Am. Chem. Soc.* **1995**, *117*, 6447.
(21) Gascoin, F.; Sevov, S. C. *J. Am. Chem. Soc.* **2000**, *122*, 10251.
(22) Klemm, M.-T.; Vaughey, J. T.; Harp, J. G.; Corbett, J. D. *Inorg. Chem.* **2001**, *40*, 7020.
(23) Rodriguez-Fortea, A.; Canadell, E. *Inorg. Chem.* **2003**, *42*, 2759.